J Therm Anal Calorim (2015) 120:847–853
DOI 10.1007/s10973-014-3802-7

Synthesis and DSC study a new pyridinedicarboximide diones derivatives, obtained under various conditions

Edward Krzyżak · Dominika Szkatuła · Berenika Szczęśniak-Sięga · Wiesław Malinka

Received: 22 November 2013 / Accepted: 27 March 2014 / Published online: 27 April 2014

Abstract The series of three 4-alkoxy-2-[2-hydroxy-3-(4-aryl-1-piperazinyl)propyl]-6-methyl-1H-pyrrolo[3,4-c] pyridine-1,3(2H)-diones were synthesized. The structures of all formed compounds were identified by elemental analysis, FTIR, and ^{1}H NMR. The synthesized compounds were studied using differential scanning calorimetry and thermogravimetric analysis in order to determine the existence of multiple solid-state forms. Our measurements showed that the solvent, mechanical treatment, and quenching are the important factors. Two stable and one metastable modification were detected. Additionally, DFT calculations were performed.

Keywords DSC · TG · Pyridinedicarboximide · Thermal analysis · DFT · Synthesis

Introduction

The chemical structure of cyclic imides arouses great interest in the scientific environment, as it creates the perfect base for the creation of new groups of derivatives. Most of the obtained derivatives can be characterized by anticonvulsant, anxiolytic, serotoninergic, and antidepressive or antibacterial activities. Moreover, many of the imides compounds show local anesthetic, analgetic, and antiinflammatory properties. Some of the derivatives are also inhibitors of the enzymes that are important in physiological processes e.g., AR-aldose reductase or caspase-3 (inhibitors of caspase-3 have been described as promising cardioprotectants, neuroprotectants, and antiarthritic agents) [1–7].

Some of the alkyl(heteroaryl)piperazinylalkyl derivatives of cyclic imides show "pure" anxiolytic activity, e.g., Buspirone. These properties are the effect of their affinity to 5-HT_1 receptor type. In order to obtain further information concerning the correlation between chemical structure and biological effects, many of the N-aminoalkyl derivatives of 3,4-pyridinedicarboximides were synthesized. Some of them were tested in the pharmacological screening test, and they have showed both the analgesic and antidepressant activities, but not the anxiolytic ones [8]. Some of these derivatives significantly suppress spontaneous locomotor activity in mice, cause hypothermia in normothermic mice, significantly decrease their amphetamine-induced hyperactivity as well as display weak analgesic action [9]. During the further research on these derivates, the structure of 1H-pyrrolo[3,4-c]pyridine-1,3(2H)-diones have been modified. These changes include mainly the introduction of alkoxy ($–OCH_3$ or $–OC_2H_5$) groups in the position two of pyridine ring (Fig. 1) and of trifluoromethyl or methoxy groups into the phenyl at N-4 of piperazine (Fig. 1, compound 2, 3). Pharmacological studies indicate that after those modifications, new compounds revealed weaker analgetic activity. In this paper, it is studied that the derivatives of 4-alkoxy-2-[2-hydroxy-3-(4-aryl-1-piperazinyl)propyl]-6-methyl-1H-pyrrolo[3,4-c]pyridine-1,3(2H)-diones (Fig. 1) are non-toxic ($LD_{50} > 2{,}000$ mg kg^{-1}) with very strong analgesic properties. In the "hot plate" test, the compounds have showed more potent analgesic activity than the acetylsalicylic acid (ED_{50} 11.9–96.8 mg kg^{-1}, for ASA 266.7 mg kg^{-1}). Also in the second test—"writing syndrome" have displayed

E. Krzyżak (✉)
Department of Inorganic Chemistry, Wrocław Medical University, ul. Borowska 211a, 50-556 Wrocław, Poland
e-mail: edward.krzyzak@gmail.com; edward.krzyzak@umed.wroc.pl

D. Szkatuła · B. Szczęśniak-Sięga · W. Malinka
Department of Chemistry of Drugs, Wrocław Medical University, ul. Borowska 211, 50-556 Wrocław, Poland

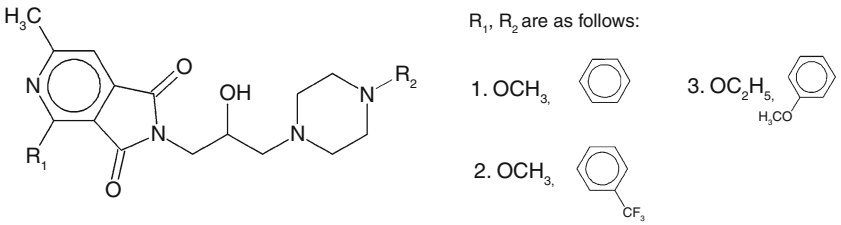

Fig. 1 *1*: 4-methoxy-2-[2-hydroxy-3-(4-phenyl-1-piperazinyl) propyl]-6-methyl-1H-pyrrolo [3,4-c] pyridine-1,3(2H)-dion, *2*: 4-methoxy-2-[2-hydroxy-3-(4-/m-trifluorophenyl-1-piperazinyl) propyl]-6-methyl-1H-pyrrolo [3,4-c] pyridine-1,3(2H)-dion, *3*: 4-ethoxy-2-[2-hydroxy-3-(4-/o-methoxyphenyl-1-piperazinyl) propyl]-6-methyl-1H-pyrrolo [3,4-c] pyridine-1,3(2H)-dion

strong analgesic activity (ED_{50} 0.4–1.35 mg kg^{-1}). It has been interesting to observe that in this test, the investigated imides have displayed superior activity to that, presented by ASA and Morphine (two reference substances—ED_{50} for ASA was 39.15 and for Morphine −2.44 mg kg^{-1}) [10, 11].

On other hand, solid form diversity of pharmaceutical substances may influence the efficacy and safety of drug products. Physical and chemical characterization of different solid phases that may occur during crystallization and pharmaceutical formulation processes, i.e. polymorphs, pseudopolymorphism, solvates, desolvated solvates, and amorphous materials, are advisable for both drugs and excipients. It is very important to control the crystal form of the drug during the various stages of drug development, because any phase changes and difference in the degree of crystallinity can alter the bioavailability of the drug.

Thermal analysis is one of the most frequently used instrumental techniques on pharmaceutical researches [12–16]. It is combined with other techniques, such as FTIR, NMR, and XRD [17–23]. The main concept of this work is to determine the thermal properties of three derivatives of 3,4-pyridinedicarboximides (slightly differ in molecular structure).

Experimental

Materials

The series of three 4-alkoxy-2-[2-hydroxy-3-(4-aryl-1-piperazinyl)propyl]-6-methyl-1H-pyrrolo[3,4-c]pyridine-1,3(2H)-diones were synthesized (Fig. 1). The starting materials for the synthesized were 4-methoxy- and 4-ethoxy-6-methyl-1H-pyrrolo [3, 4] pyridine-1,3(2H)-diones. Details of preparation are given in Ref. [10]. The final compounds were crystallized from ethanol and toluene. Verification of the obtained compounds was carried out by elemental analysis, IR, and ^{1}H NMR spectroscopy. ^{1}H NMR spectra was obtained on a Tesla 587 A spectrometer (80 MHz), when not indicated otherwise, using TMS as an internal standard.

For NMR spectroscopy, the samples were prepared by dissolving 5 mg of each form in 600 µl of $CDCl_3$. The NMR spectra all four compounds have characteristic signals of piperazine, benzene, and other protons. In NMR spectrum of compound 1, we can see multiple signals of piperazine four protons, three protons from CH_3 (at 6-metylo), and two protons from $–CH_2$ at 2.47–2.82 ppm (m-9H, CH_3, $–CH_2–N(CH_2)_2$-). Other four protons from piperazine are observed in signal at 3.13–3.25 ppm (t-4H, $-(CH_2)_2–$N-benzene). Signals from two protons of H_α-propyl are observed at 3.73–3.80 ppm (d-2H, $-CH_2$ of propyl). Multiple signals from OCH_3 and H_β-propyl and hydroxy group are recorded at 3.80–4.30 ppm (m-5H, OCH_3, -CH of propyl, -OH). And finally, multiple signals of benzene's five protons and one proton from pyridine at 6.85–7.26 ppm are observed (m-6H, m-5H, arom., 1H pyridine).

In NMR spectrum of compound 2, we can see multiple signals of piperazine four protons, three protons from CH_3 (at 6-metylo), and two protons from $–CH_2$ at 2.45–2.70 ppm (m-9H, CH_3, $–CH_2–N(CH_2)_2$-). Other four protons from piperazine are observed in signal at 3.00–3.20 ppm (t-4H, $–(CH_2)_2–N–C_6H_4–m–CF_3$). Signals from two protons of H_α-propyl are observed at 3.73–3.80 ppm (d-2H, $–CH_2$ of propyl). Multiple signals from OCH_3 and H_β-propyl and hydroxy group are recorded at 3.85–4.12 ppm (m-5H, OCH_3, –CH of propyl, –OH). And finally, multiple signals of benzene's four protons and one proton from pyridine at 7.08–7.43 ppm are observed (m-5H, arom., 1H pyridine).

In NMR spectrum of compound 3, we can see signal from three protons of –ethoxy group at 1.43–1.47 ppm (t-3H, $-OCH_2CH_3$). Multiple signals of piperazine four protons, three protons from CH_3 (at 6-metylo), and two protons from $–CH_2$ are observed at 2.57–2.71 ppm (m-9H, CH_3, $–CH_2–N(CH_2)_2$-). Other four protons from piperazine are observed in signal at 2.75–2.99 ppm (t-4H, $–(CH_2)_2–N–C_6H_4–o–OCH_3$). Multiple signals from OCH_3, Hα, and $2H_\beta$-propyl and hydroxy group (m-7H, –CH–CH_2, –OH, $-C_6H_4–o–OCH_3$) at 3.82–4.04 ppm and signal from two protons of -ethoxy group are also recorded (d-2H,

–OCH_2CH_3). And finally, multiple signals of benzene's four protons and one proton from pyridine at 6.80–7.15 ppm are observed (m-4H, arom., 1H pyridine).

Elemental analyses were run on a Carlo Erba NA 1500 analyser, and the results were within ±0.4 % of the values calculated for the corresponding formulas. Elemental analysis confirms these free structures: compound 1 $C_{22}H_{26}N_4O_4$: found: C, 66.43 %; H, 6.37 %; N, 13.70 % (analytical: C, 64.39 %; H, 6.34 %; N, 13.66 %.), compound 2 $C_{23}H_{25}F_3N_4O_4$: found: C, 57.45 %; H, 5.39 %; N, 11.38 % (analytical: C, 57.74 %; H, 5.23 %; N, 11.72 %.), and compound 3 $C_{24}H_{30}N_4O_5$: found: C, 63.85 %; H, 6.42 %; N, 12.68 % (analytical: C, 63.44 %; H, 6.61 %; N, 12.33 %.).

Thermal analysis

The DSC traces were recorded on a Mettler Toledo DCS 25 measuring cell with TC15 TA Controller, calibrated with indium to ensure the accuracy of the calorimetric scale. Samples weighing 8–12 mg were characterized in sealed 40 μL aluminum pans with lids and subjected to thermal analysis under a flowing argon atmosphere (30 cm^3 min^{-1}). Analysis was carried out from room temperature to about 20–30 degree above melting temperature using heating rates of 5 K min^{-1} with an identical empty sample pan as reference. The heat flow versus temperature scans have been measured for samples obtained from ethanol and toluene, after shock cooling and after mechanical treatment. Thermogravimetric analysis was performed by TG50 with Mettler Toledo Star^e System. The samples were placed in open alumina crucibles and heating at the rate of 5 K min^{-1} under flowing argon atmosphere (30 cm^3 min^{-1}).

FTIR

FTIR spectra were run on a Perkin-Elmer Spectrum Two UATR FT-IR spectrometer. The samples were applied as solids. Each spectrum was derived from 16 single averaged scans collected in the region 450–4,000 cm^{-1} at a spectral resolution of 2 cm^{-1}.

Computational methods

Calculations were carried out using the GAUSSIAN 09 software package [24]. Density Functional Theoretical (DFT) computations were performed using the closed shell Becke–Lee–Yang–Parr hybrid exchange–correlation three-parameter functional (B3LYP) [25–27] in combination with 6-311 + G (d,p) basis set.

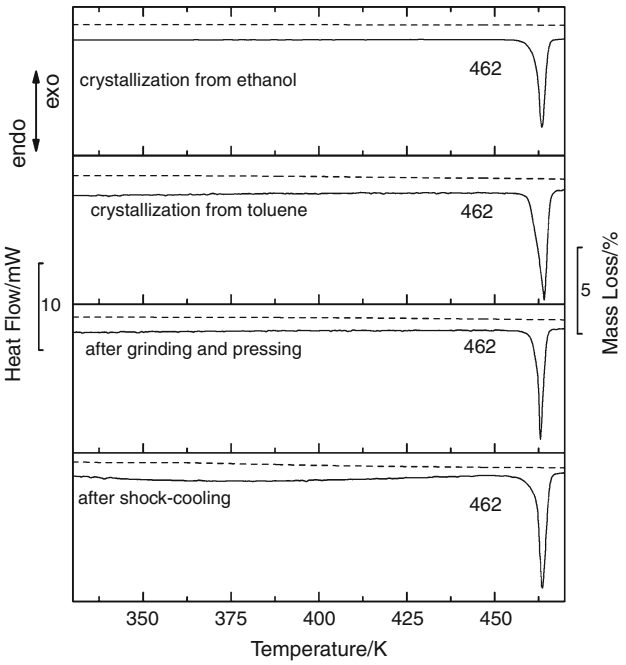

Fig. 2 DSC (*solid*) and TG (*dash*) traces at 5 K min^{-1} for compound 1

Results and discussion

Studies on the thermal properties have been performed by differential scanning calorimetry (DSC) and thermogravimetric analysis (TG). At the beginning, heat flow versus temperature scans has been measured for samples obtained from ethanol and toluene. In accordance with Ostwald's rule, the less stable modifications are often formed first on the crystallizing process from the melt. These rearranged then stepwise to the stable form. Quite often, it is easier to obtain metastable forms by slowly heating amorphous material (obtained by shock cooling from the melt) above the glass transition temperature [28]. This procedure was carried out next for all compounds. Sometimes metastable form may be also generated by mechanical treatment. After crystallization from ethanol, samples were grinded in a mortar pestle, pressed, and then DSC experiment was made. Additionally to determinate absence of solvates or decomposition, the TG measurements were carried out.

The DSC scans for compound 1 are shown in Fig. 2. For all runs, only one endothermic thermal effect, corresponds to the melting, is observed. Temperature values are 462 K (crystallization from ethanol), 462 K (crystallization from toluene), and 462 K (after grinding and pressing). After a shock cooling, the second measurement was carried out. DSC trace shows only endothermic peak at 462 K. In TG analysis, for all samples, no mass loss has indicated the absence of solvate and decomposition process in investigation temperature range (Fig. 2).

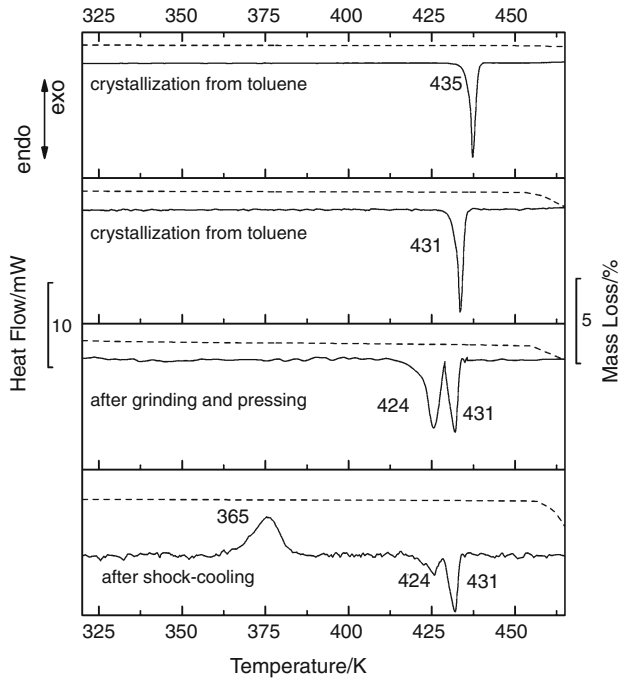

Fig. 3 DSC (*solid*) and TG (*dash*) traces at 5 K min^{-1} for compound 2

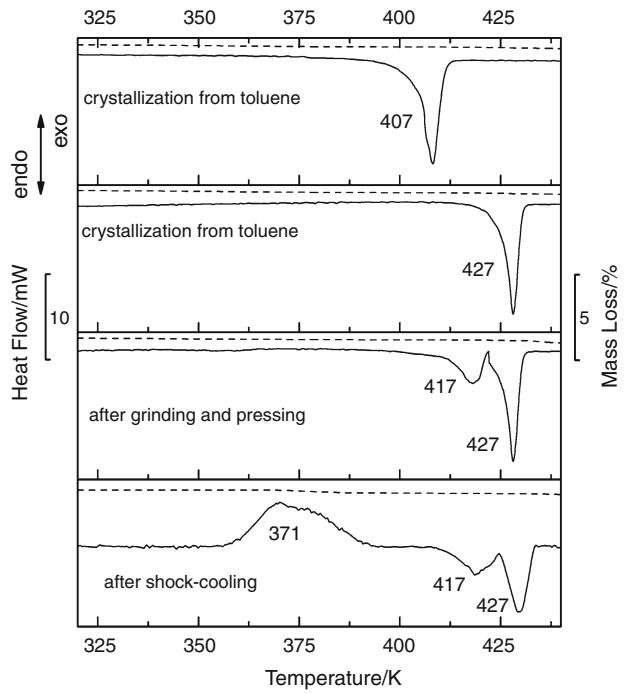

Fig. 4 DSC (*solid*) and TG (*dash*) traces at 5 K min^{-1} for compound 3

The DSC scans for compound 2 are shown in Fig. 3. For a first heating run, only one endothermic thermal effect is observed. The temperature differs slightly, depending on the type of sample. The melting temperature is 435 K for sample crystallized from ethanol, 431 K for sample crystallized from toluene. For sample which was grinded and pressed, two thermal effects are observed: at 424 and 431 K. After a shock cooling and heating again, three thermal effects are detected a single exothermic peak at 365 K due to cold crystallization and two endothermic peaks at 424 and 431 K. In TG analysis, for all samples, no mass loss up to 25 degree above melting temperature has indicated the absence of solvate (Fig. 3). At higher temperature (above melting), the decomposition is started.

The DSC scans for compound 3 are shown in Fig. 4. One endothermic peak has been detected at 407 K (crystallization from ethanol). For the sample crystallized from toluene, the melting point is several degrees higher. The value is 427 K. For sample which was grinded and pressed, two thermal effects are observed: at 417 and 427 K. After a shock cooling and heating again, the DSC trace shows exothermic peak at 371 K (cold crystallization). On further heating, two exothermic peaks, at 417 and 427 K, are observed. In TG analysis, for all samples, no mass loss has indicated the absence of solvate and decomposition process in investigation temperature range (Fig. 4).

The FTIR spectra for all compounds are shown in Figs. 5, 6, and 7. All molecules contain two imide carbonyl groups and one hydroxy group. For compound 1, FTIR spectra for various samples are identical (Fig. 5). The carbonyl groups are recorded at 1,725 and 1,770 cm^{-1}. The stretching vibration of the hydroxyl group is observed at 3,380 cm^{-1}. In the FTIR spectra of compound 2 (Fig. 6), there are major differences between the spectra of samples. In the region 3,500–2,600 cm^{-1}, weak and broad bands are observed. For the sample crystallized from toluene, a small peak at 3,375 cm^{-1} is observed. This can be assigned to stretching vibration of the hydroxyl group. For samples crystallized from ethanol and after mechanical treatment, weak and broad bands are assigned to stretching vibration of the hydroxyl group involved in the hydrogen bonding, which is superimposed on the C–H and Ar–H stretching vibration. In the region 2,600–450 cm^{-1}, the spectra of three forms are reasonable similar. The carbonyl groups are recorded at 1,720–1,770 cm^{-1}. Small differences are observed between 1,250 and 1,000 cm^{-1}. Also for compound 3 in the region 3,500–2,600 cm^{-1}, there are major differences between spectra of samples (Fig. 7). For the sample crystallized from toluene, a small peak at 3,190 cm^{-1} is observed (–OH stretching vibration). For other forms, hydroxyl group can be involved in H bonding. In the region 2,600–450 cm^{-1}, the spectra of three forms are reasonably similar. The carbonyl groups are recorded at 1,722–1,775 cm^{-1}. Small differences are observed between 1,400 and 1,150 cm^{-1}.

Our results show that the type of solvent used for crystallization is an important factor. Pseudopolymorphism

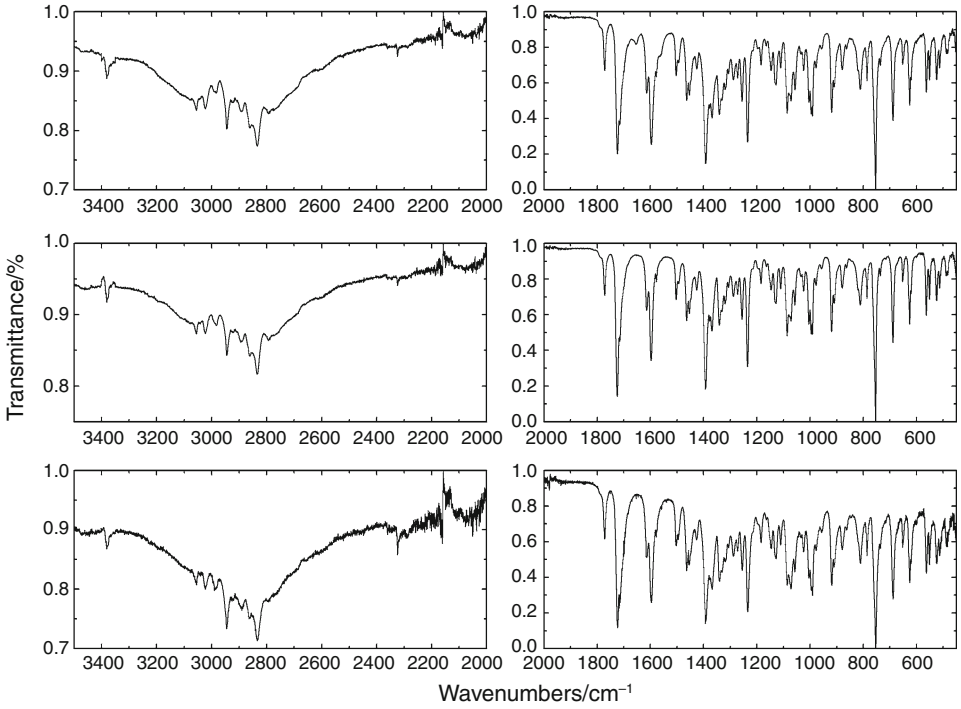

Fig. 5 Experimental FTIR spectrum for various samples of compound 1: crystallization from ethanol, crystallization from toluene, after mechanical treatment (from *top* to *bottom*)

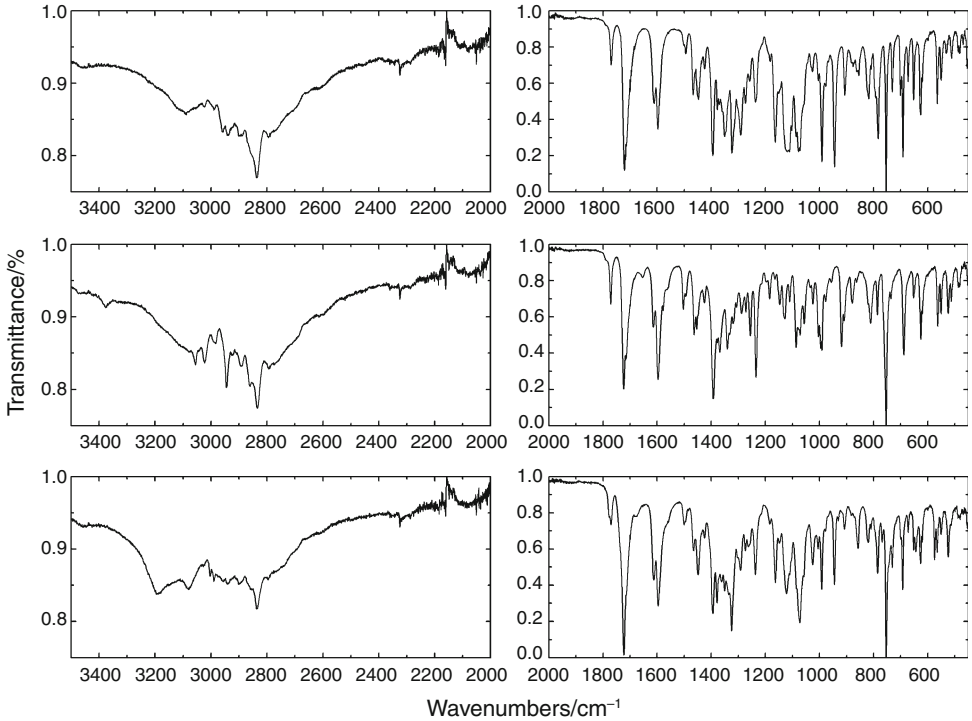

Fig. 6 Experimental FTIR spectrum for various samples of compound 2: crystallization from ethanol, crystallization from toluene, after mechanical treatment (from *top* to *bottom*)

exists crystalline forms of a compound in which the solvent molecules are included as an integral part of the structure, is well known is in pharmaceutical industry. It should be expected that packing of crystal may be different in polar and nonpolar (ethanol and toluene) solvents or interaction with ethanol molecules. However, it is interesting that the solvent effect is not observed for compound 1.

We made a theoretical calculation of energy of interaction between title compounds and ethanol molecule. Calculations were carried out for positions where it is

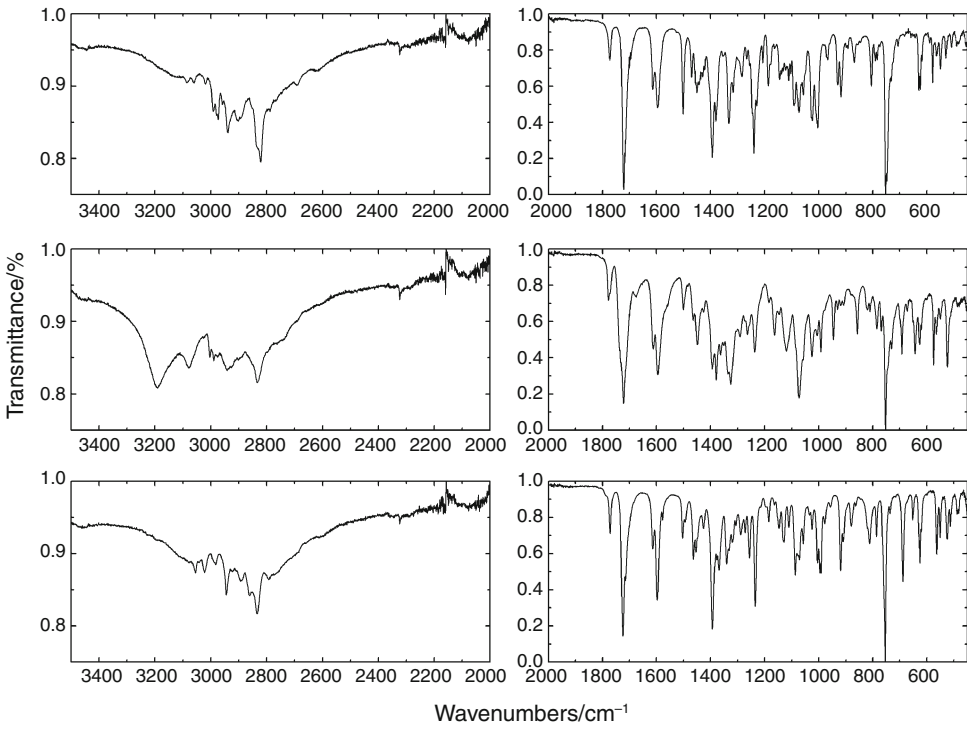

Fig. 7 Experimental FTIR spectrum for various samples of compound 3: crystallization from ethanol, crystallization from toluene, after mechanical treatment (from *top* to *bottom*)

possible hydrogen bonding. The calculations show that for compound 1, energy of interaction is positive: +2.3 to +2.53 kcal mol^{-1}. For compounds 2 and 3, molecules with substituted pyridine ring, energy of interaction via a hydrogen bond is negative: −5.0 to −5.3 kcal mol^{-1} (compound 2) and −4.7 to −5.13 kcal mol^{-1} (compound 3). The distance between EtOH···O is relatively short: 1.82–1.95 Å. Those results may indicate a high probability of the intermolecular hydrogen bonding for molecules with substituted pyridine ring.

Our results also indicate that compounds with substituted pyridine ring occur in three forms. Modification 1 is formed during crystallization from ethanol. Modification 2 is formed during crystallization from toluene. Metastable form 3 is formed after grinding and pressing and after shock cooling and leads to stable form 2.

Conclusions

Three derivatives of 4-alkoxy-2-[2-hydroxy-3-(4-aryl-1-piperazinyl)propyl]-6-methyl-1H-pyrrolo[3,4-c]pyridine-1,3(2H)-diones were synthesized. The studied compounds are the interesting materials due to their analgesic activity. The differential thermal analysis (DSC) has been used to solid-state characterization. Additionally, Density Functional Theoretical (DFT) computations were performed. In pharmaceutical industry, it is very important to control the purity of crystal form. The aspect of our investigation was to determine the existence of multiple solid-state forms. Our measurements showed that the solvent, grinding, pressing, and quenching are the important factors. It seems that a compound 1 (with unsubstituted phenyl in phenylpiperazine ring) probably exits in only one form. The m-substituted derivative (compound 2) and the o-substituted derivative probably occurs in two stable forms, crystalized from ethanol and toluene, and metastable modification, formed after during mechanical treatment and after shock cooling. The theoretical calculation shows that only for compound 2 and 3, it is possible for hydrogen bonding with ethanol solvent.

Acknowledgements Calculations have been carried out in the Wroclaw Centre for Networking and Supercomputing (http://www.wcss.wroc.pl).

References

1. Kossakowski J, Raszkiewicz A, Bugno R, Bojarski AJ. Introduction of a new complex imide system into the structure of LCAPs. The synthesis and a 5-HT1A, 5-HT2A and D2 receptor binding study. Pol J Pharmacol. 2004;56:843–8.
2. Bojarski AJ, Mokrosz MJ, Duszyńska B, Kozioł A, Bugno R. New imide 5-HT1A receptor ligands—modification of terminal fragment geometry. Molecules. 2004;9:170–7.

3. Nowak M, Kołaczkowski M, Pawłowski M, Bojarski AJ. Homology modelling of the serotonin 5-HT1A receptor using automated docking of bioactive compounds with defined geometry. J Med Chem. 2006;49:205–14.
4. Da Settimo F, Marini DM, Motta CL, Simorini F, Lucheti E, Bertini S. Synthesis and local anaesthetic activity of some 7-amino-2-dialkylaminoalkylpyrrolo[3,4-c] pyridine derivatives. Farmaco. 1996;51:725–8.
5. Da Settimo A, Primofiore G, Da Settimo F, Simorini F, La Motta C, Martinelli A, Boldrini E. Synthesis of pyrrolo[3,4-c]pyridine derivatives possessing an acid group and their in vitro and in vivo evaluation as aldose reductase inhibitors. Eur J Med Chem. 1996;31:49–58.
6. Cobo J, Sanchez A, Nogureras M, DeClercq E. Synthesis and antiviral evaluation of pyridine fused heterocyclic and nucleosidic derivatives. Tetrahedron. 1997;53(24):8225–36.
7. Kravchenko DV, Kysil VV, Tkachenko SE, Maliarchouk S, Okun IM, Ivachtchenko AV. Pyrrolo[3,4-c]quinoline-1,3-diones as potent caspase-3 inhibitors. Synthesis and SAR of 2-substituted 4-methyl-8-(morpholine-4-sulfonyl)-pyrrolo[3,4-*c*]quinoline-1,3-diones. Eur J Med Chem. 2005;40:1377–83.
8. Śladowska H, Dereń-Wesołek A. Investigations on the synthesis and properties of some N-heteroarylpiperazinylalkyl derivatives of imides of 3,4-pyridinedicarboxylic acids. Farmaco. 1993;48(6): 827–34.
9. Śladowska H, Sieklucka-Dziuba M, Misztal M, Kleinrok Z. Investigations on the synthesis and properties of n-aryl (heteroaryl) piperazinylalkyl derivatives of imide of 6-methyl-2-(1-piperidino)-3,4-pyridinedicarboxylic acid. Farmaco. 1994;49(7–8):493–8.
10. Śladowska H, Filipek B, Szkatuła D, Sabiniarz A, Kardasz M, Potoczek J, Sieklucka-Dziuba M, Rajtar G, Kleinrok Z, Lis T. Investigations on the synthesis and pharmacological properties of 4-alkoxy-2-[2-hydroxy-3-(4-aryl-1-piperazinyl)-propyl]-6-methyl-1H-pyrrolo[3,4-c]pyridine-1,3(2H)-diones. Farmaco. 2002;57: 897–908.
11. Śladowska H, Filipek B, Szkatuła D, Sapa J, Bednarski M, Ciołkowska M. Investigations on the synthesis and pharmacological properties of N-substituted derivatives of 4-alkoxy-6-methyl-1H-pyrrolo[3,4-c]pyridine-1,3(2H)-diones. Farmaco. 2005;60:53–9.
12. Ford JL, Timmins P. Pharmaceutical thermal analysis: techniques and applications. New York: Wiley; 1989.
13. Haines PJ. Thermal. In: Kopsch H, editor. Methods of analysis—principles, applications and problems. London: Blackie Academic and Professional; 1995.
14. Charsley EL, Warrington SB. Thermal analysis: techniques and applications. Cambrigde: Royal Society of Chemistry; 1992.
15. Craig Duncan QM, Reading M. Thermal analysis of pharmaceuticals. Boca Raton: CRC Press; 2007.
16. Giron D. Applications of thermal analysis and coupled techniques in pharmaceutical industry. J Therm Anal Cal. 2002;68(2): 335–57.
17. Vyas PM, Pansuriya AM, Naliapara YT, Joshi MJ. Spectroscopic, thermal, and dielectric studies of n-butyl 4-(3,4-dimethoxyphenyl)-6-methyl-2-thioxo-1,2,3,4 tetrahydropyrimidine-5-carboxylate crystals. J Therm Anal Cal. 2013;114(2):839–44.
18. Fulias A, Vlase G, Grigorie C, Ledeţi I, Albu P, Bilanin M, Vlase T. Thermal behaviour studies of procaine and benzocaine. J Therm Anal Cal. 2013;113(1):265–71.
19. Tita B, Jurca T, Tita D. Thermal stability of pentoxifylline: active substance and tablets. J Therm Anal Cal. 2013;113(1):291–9.
20. Ikeda H, Sano Y, Matsubara T, Kawahara M, Yukawa M, Fujisawa M, Yukawa E, Aki H. Drug–tea polyphenol interaction. J Therm Anal Cal. 2013;113(3):1135–8.
21. Vlaicu ID, Constand M, Olar R, Marinescu D, Grecu MN, Lazar V, Chifiriuc MC, Badea M. Thermal stability of new biologic active copper (II) complexes with 5,6-dimethylbenzimidazole. J Therm Anal Cal. 2013;113(3):1369–77.
22. Chilwal A, Malhotra P, Narula AK. Thermal analysis of new dimethyl/dibutyl tin (IV) compounds with amino acids. J Therm Anal Cal. 2013;114(1):345–51.
23. Krzyżak E, Szczęśniak-Sięga B, Malinka W. Synthesis and thermal behaviour of new benzo-1,2-thiazine long-chain arylpiperazine derivatives. J Therm Anal Cal. 2014;115(1):793–802.
24. Frisch MJ, Trucks GW, Schlegel HB, Scuseria GE, Robb MA, Cheeseman JR, Scalmani G, Barone V, Mennucci B, Petersson GA, Nakatsuji H, Caricato M, Li X, Hratchian HP, Izmaylov AF, Bloino J, Zheng G, Sonnenberg JL, Hada M, Ehara M, Toyota K, Fukuda R, Hasegawa J, Ishida M, Nakajima T, Honda Y, Kitao O, Nakai H, Vreven T, Montgomery JA Jr, Peralta JE, Ogliaro F, Bearpark M, Heyd JJ, Brothers E, Kudin KN, Staroverov VN, Kobayashi R, Normand J, Raghavachari K, Rendell A, Burant JC, Iyengar SS, Tomasi J, Cossi M, Rega N, Millam JM, Klene M, Knox JE, Cross JB, Bakken V, Adamo C, Jaramillo J, Gomperts R, Stratmann RE, Yazyev O, Austin AJ, Cammi R, Pomelli C, Ochterski JW, Martin RL, Morokuma K, Zakrzewski VG, Voth AG, Salvador P, Dannenberg JJ, Dapprich S, Daniels AD, Farkas O, Foresman JB, Ortiz JV, Cioslowski J, Fox DJ. Gaussian 09 Revision C.02. Wallingford: Gaussian Inc; 2009.
25. Becke AD. Density-functional thermochemistry. III. The role of exact exchange. J Chem Phys. 1993;98:5648–53.
26. Lee C, Yang W, Parr RG. Development of the Colle-Salvetti correlation energy formula into a functional of the electron density. Phys Rev. 1988;B37:785–9.
27. Perdew JP, Wang Y. Accurate and simple analytic representation of the electron-gas correlation energy. Phys Rev. 1992;45:13244–9.
28. Giron D. Thermal analysis and calorimetric methods in the characterisation of polymorphs and solvates. Thermochim Acta. 1995;248:1–59.